



Novel method to prepare sodium chromate from carbon ferrochrome

Jia-liang WANG, Guo-rong HU, Zhong-dong PENG, Ke DU

School of Metallurgy and Environment, Central South University, Changsha 410083, China

Received 12 January 2015; accepted 19 May 2015

Abstract: An oxidizing roasting process of carbon ferrochrome to prepare sodium chromate in the presence of sodium carbonate and air was investigated. The effects of reaction temperature, reaction time, mole ratio of sodium carbonate to carbon ferrochrome were studied, and thermodynamics and kinetics of the reaction were also discussed. It was observed that there was a sudden increase in reaction rate when the temperature rose to a certain value, and the sample with a smaller grain size could start the sudden increase at a lower temperature. The chromium recovery rate increased with the increase of mole ratio of sodium carbonate to carbon ferrochrome, and it reached up to 99.34% when mole ratio of sodium carbonate to carbon ferrochrome increased to 1.2:1. The chromium residue yielded from this method was only about 1/3 of the product. Moreover, the content of Fe in the residue was as high as 60.41%. Therefore, it can be easily recovered to produce sponge iron, realizing complete detoxication and zero-emission of chromium residue.

Key words: carbon ferrochrome; sodium chromate; oxidizing roasting; chromium residue; zero-emission

1 Introduction

Chromate compounds are important chemical products, which have been widely used in metallurgy, chemistry, material and leather-making. Normally, the chromate products are achieved via a soda–ash roasting process, which is now under enormous pressure due to the environmental problems [1]. In this soda–ash roasting process, lime with about 100% (mass fraction) of the chromite ore was incorporated in the charge to control the siliceous and acid gangue minerals in the ore. But the addition of lime generates a large quantity of highly alkaline chromite ore processing residue (COPR), which contains hexavalent chromium of 1%–2% (mass fraction). It also results in the generation of CaCrO_4 , which is volatile and airborne, causing a major threat to human, animal, and plant health. The remediation of the COPR is either too expensive or not thorough [2,3]. Although the lime-free roasting process can reduce the COPR and restrict the generation of CaCrO_4 , the necessity for high grade chromite ores with silica content of less than 1% restricts its wide application [4].

Carbon ferrochrome (CrFeC) is a kind of intermediate product of chromium metallurgy, which is

mainly used for producing stainless steel, tool steel, ball-bearing steel, heat resistant steel, and so on [5]. CrFeC is produced from chromite ore through a electric furnace reduction process, and thanks to the strong reducing atmosphere, the slag yielded from this process has no hexavalent chromium, therefore, it nearly has no threat to the environment. Because the factories for producing CrFeC are always built in areas where electric power and mineral resources are rich, there are only fewer economic disadvantages using CrFeC as raw material than using chromite ore. Accordingly, a novel method to prepare Na_2CrO_4 from CrFeC through an oxidizing roasting process was proposed. The residue emitted from this process was very little, and mainly consisted of iron oxides, which could be easily recovered to produce sponge iron. Therefore, the target of zero-emission of chromium residue can be realized, and the chromium residue pollution problem can be resolved completely.

2 Experimental

CrFeC specimen originated from Africa was provided by Jiafei New Material Co., Ltd., Hunan Province, China. The particle size of the CrFeC

specimen is 12.6 μm (median diameter). The chemical components and the phase compositions are shown in Table 1 and Fig. 1, respectively.

Table 1 Chemical components of CrFeC (mass fraction, %)

Cr	Na	Fe	S	C
60.6	0.013	27.9	5.0×10^{-3}	8.7
Mn	V	Mg	Pb	Co
1.9	0.06	0.12	3.2×10^{-3}	0.14
Si	Ni	Al	Ti	
0.24	0.11	0.14	0.095	

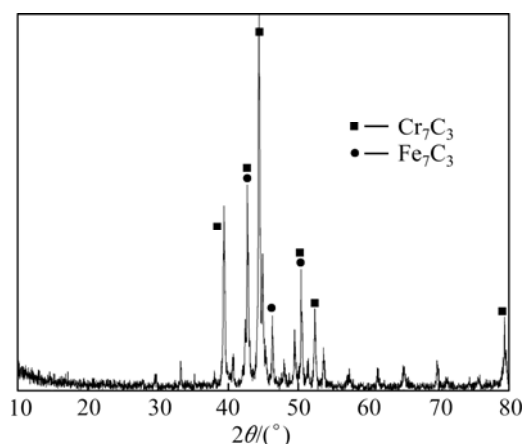
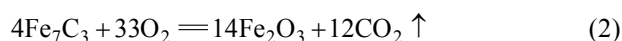
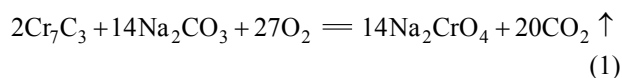


Fig. 1 XRD pattern of CrFeC

According to the chemical analysis results in Table 1 and the XRD pattern in Fig. 1, the main components of CrFeC are Cr_7C_3 and Fe_7C_3 . During the roasting process, Cr_7C_3 is oxidized to Na_2CrO_4 in the presence of O_2 and Na_2CO_3 , while the component of Fe_7C_3 is converted to Fe_2O_3 . The equations of the main reactions are as follows [6]:



The experiments were carried out in a muffle furnace. Temperature was precisely controlled by a programming temperature controller. CrFeC was mixed homogeneously with a certain amount of Na_2CO_3 in a porcelain mortar. Then, the mixture was loaded in a corundum boat and put into the muffle furnace when temperature of the muffle furnace rose to the specified value. When time was up, the roasted product was taken out and cooled quickly. The roasted product was leached in distilled water at 313 K with the liquid-to-solid ratio of 5:1 (mass fraction), and then washed three times under the same condition. At last, it was filtered to get a chromate solution and a solid residue. The solution was analyzed for Cr and other impurities. The conversion rate

was calculated according to the following formula:

$$r = \frac{m_r}{m_o} \times 100\% \quad (3)$$

where r is the conversion rate of Cr; m_r is the total quantity of Cr in the solution and m_o is the total quantity of Cr in CrFeC. While the residue was analyzed for Cr(VI) to determine the quantity of Cr(VI) remaining in the residue.

The leaching solution was analyzed by inductively coupled plasma-optical emission spectrometer (ICP-OES, PE Optima 5300DV, Perkin Elmer), and the residues were analyzed with a volumetric titration method. The phase identification was carried out on an X-ray diffraction (XRD, Phillips PW223/30). The particle size distribution was measured by a particle size analyzer (LS230, Beckman, Coulter). SEM (scanning electron microscopy) images were taken on a JSM-35CF SEM equipment (Japan Electron Optics Laboratory Co., Ltd.). Thermoanalysis was performed on a universal V4.0C TA instrument (SDT Q600 V8.0 Build 95).

3 Results and discussion

3.1 Thermodynamical analysis

The standard Gibbs energy changes ($\Delta_r G^\ominus$) and standard enthalpy changes ($\Delta_r H^\ominus$) of Reaction (1) are shown in Figs. 2 and 3, respectively. They are calculated using the method in Ref. [7] following the assumptions below:

- 1) All the components in Reaction (1) are pure substances.
- 2) The gases of oxygen and carbon dioxide are all in standard state.
- 3) Cr_7C_3 is solid, and its activity is equal to 1. Na_2CrO_4 and Na_2CO_3 can be in liquid or solid state, depending on the roasting temperature, and their activities are equal to 1.

The highly negative values of $\Delta_r G^\ominus$ shown in Fig. 2

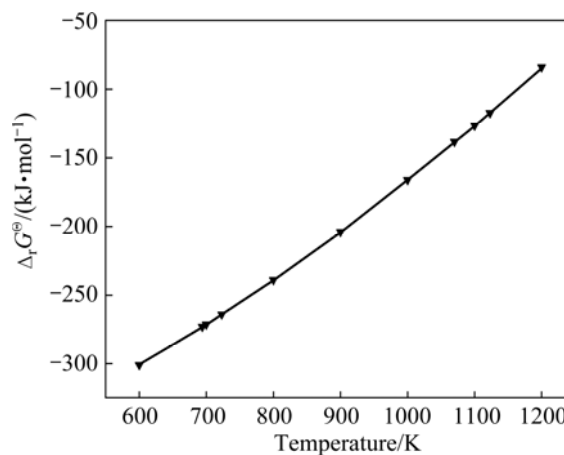


Fig. 2 $\Delta_r G^\ominus$ of Reaction (1) at 600–1200 K

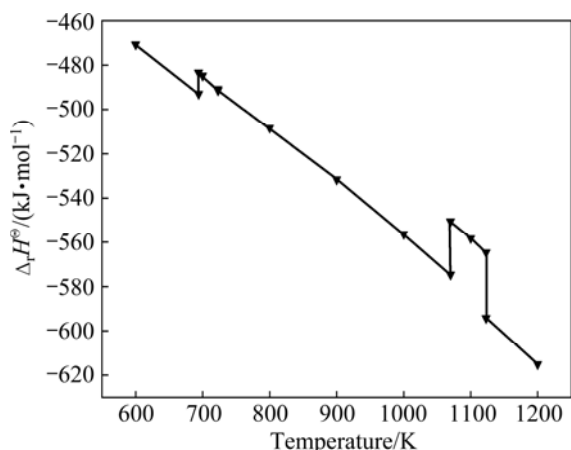


Fig. 3 $\Delta_r H^\ominus$ of Reaction (1) at 600–1200 K

indicate that Reaction (1) has a very intensive thermodynamic tendency. And the lower the temperature is, the higher the reaction tendency will be. The negative $\Delta_r H^\ominus$ values of Reaction (1) in Fig. 3 show that the oxidizing roasting reaction of CrFeC is an exothermic process, which can contribute to the reduction of energy consumption [7].

The DTA–TG analysis was employed to determine the behaviors of the reactants during the roasting process. CrFeC and Na_2CO_3 were mixed at stoichiometric ratio, and then performed in a DTA–TG instrument with a temperature rising rate of 5 K/min in air. On the DTA–TG curve in Fig. 4, the mass loss of 1.54% before 410.52 K is caused by the evaporation of the free water and chemically combined water. Between 410.52 and 908.82 K, the mass loss shows a slight rising on the TG curve, accompanied with a mass loss of 1.14%, which is induced by the slow oxidization of CrFeC. From 908.82 K, the roasting reaction is intensified suddenly, and a sharp exothermic peak is observed at 945.15 K, the corresponding mass loss is 0.44%. With increasing the temperature, Na_2CO_3 – Na_2CrO_4 eutectic melt emerges rapidly, and a significant endothermic process can be

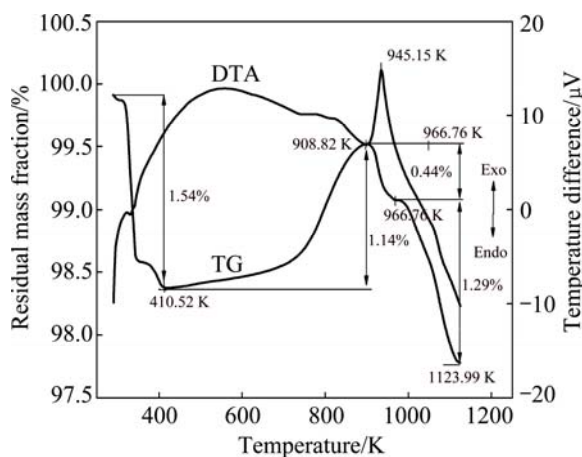


Fig. 4 DTA–TG curves of CrFeC and Na_2CO_3 mixture

seen after 966.76 K. Because the vapor pressure of Na_2CrO_4 will obviously increase after melting to liquid phase, the total mass decreases significantly due to the evaporation of Na_2CrO_4 in the temperature range from 966.76 to 1123.99 K, and the corresponding mass loss reaches up to 1.29%. It can be seen that, liquid phase of Na_2CrO_4 is easy to vaporize.

3.2 Kinetics

The conversion rates of CrFeC as a function of time at different temperatures are compared in Fig. 5. The reaction regimes are quite different as temperature changes. The eventual conversion rate increases with the rising of temperature. According to the DTA–TG plots in Fig. 4, there is no melting phenomenon at 873 and 923 K. Therefore, the reaction among CrFeC, Na_2CO_3 and O_2 is gas–solid–solid reaction. At the beginning of the reaction, quantities of the reactants are all enough, therefore, it can be assumed that the concentrations of the reactants are all invariable. According to the shrinking un-reacted core model [6,8,9], if the reaction was controlled by the interface chemical reaction, it will fit the kinetic equation $1-(1-r)^{1/3}=kt$, where r and t are conversion rate and reaction time, respectively. From Fig. 6, it can be seen that, at 873 and 923 K, the first half of the kinetic curves fit well with equation $1-(1-r)^{1/3}=kt$, namely, the roasting reaction under these conditions is controlled by interface chemical reaction. The apparent activation energy (E_a) calculated using the data in Fig. 6 by the Arrhenius equation [10] is 51.85 kJ/mol. The relatively high value of E_a gives a further proof that the process is controlled by interface chemical reaction in this temperature range.

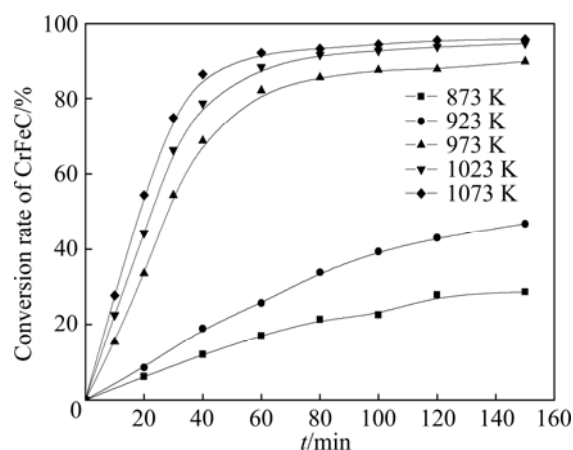


Fig. 5 Conversion rate (r) of CrFeC at various temperatures

It can be observed from the DTA–TG analysis that the Na_2CO_3 – Na_2CrO_4 eutectic melt will emerge rapidly when temperature reaches up to 973 K. So, the reaction among CrFeC, Na_2CO_3 and O_2 is gas–liquid–solid reaction. In the presence of the melt, the contact area of

the reactants increases dramatically. Moreover, CO_2 produced in the reaction process makes the reactant loose and porous. So, the reaction velocity at 973 K has a great improvement compared with that at 923 K. The relationships between conversion rate (r) and reaction time (t) at 973, 1023 and 1073 K are plotted in Fig. 7. According to the plots in Fig. 7, the relationships between conversion rate (r) and reaction time (t) are all linear at the beginning of the reaction at the three temperatures. According to the shrinking un-reacted core model, the reaction is controlled by the external diffusion process [11]. The apparent activation energy (E_a) calculated using the data in Fig. 7 by the Arrhenius equation [10] is 26.53 kJ/mol. The relatively low value of E_a gives further proof that the reaction is controlled by external diffusion process in this temperature range [12,13].

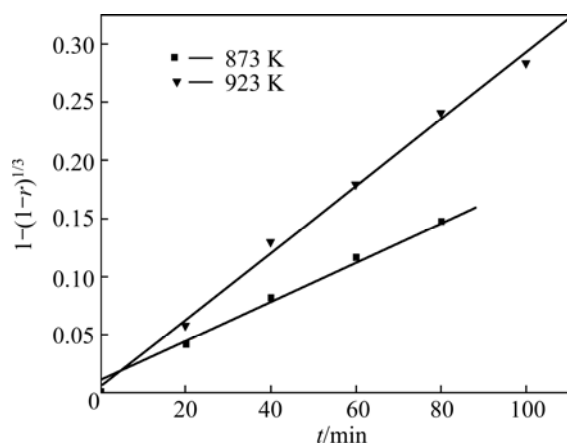


Fig. 6 Plot of $1-(1-r)^{1/3}$ versus t at 873 and 923 K

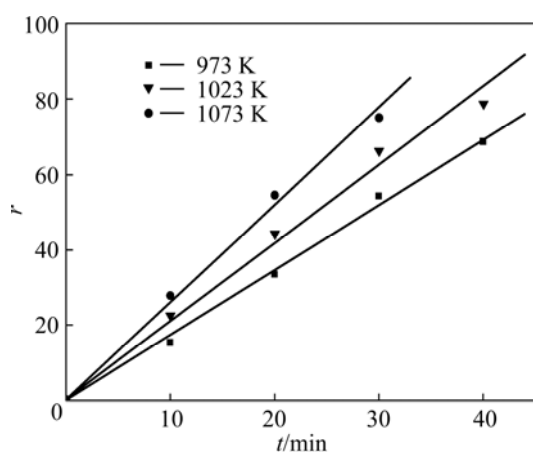


Fig. 7 Plot of r versus t at 973, 1023 and 1073 K

Figure 8 shows the XRD patterns of the leaching residues obtained at 873 and 973 K. The main components of the residue obtained at 873 K are Cr_7C_3 and $\text{Fe}\cdot 2\text{Cr}_2\text{O}_4$. With the time going, the peak intensity of Cr_7C_3 is weakened gradually, while the peak intensity of $\text{Fe}\cdot 2\text{Cr}_2\text{O}_4$ is enhanced significantly. This is because

there is nearly no melting substance at this temperature, CrFeC powder cannot be effectively covered by Na_2CO_3 , but exposes in air. So, CrFeC is oxidized by O_2 directly. At 973 K, the main components of the residue are Fe_3O_4 , Fe-Cr , and a small quantity of CrOOH . The peak intensity of Fe_3O_4 is enhanced with the prolonging of time, while that of Fe-Cr decreases. The peak intensity of CrOOH is always kept at a low level. At this temperature, a large quantity of $\text{Na}_2\text{CO}_3\text{-Na}_2\text{CrO}_4$ eutectic melt is present and large amount of CO_2 gas is produced, which not only makes the reactants loose and porous, but also makes CrFeC powder covered by the melt thoroughly. So, the conversion rate is improved significantly.

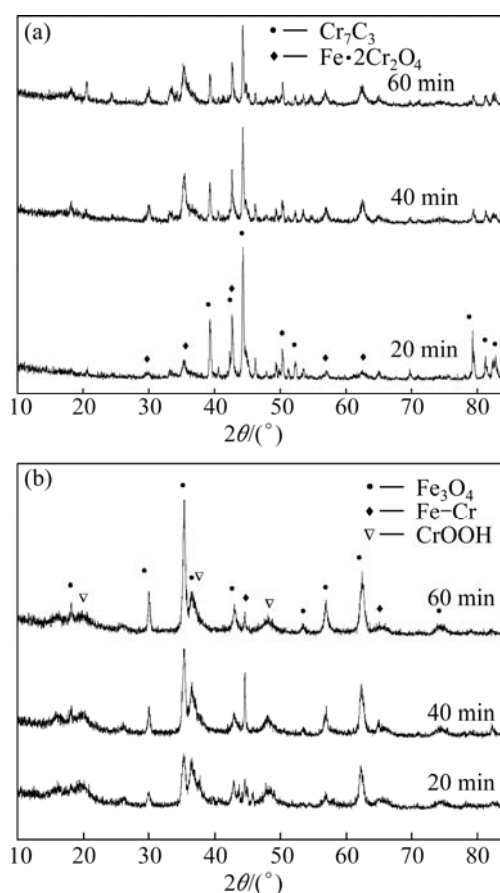


Fig. 8 XRD patterns of leaching residues obtained at different roasting temperatures: (a) 873 K; (b) 973 K

Accordingly, there will be a jump of the conversion rate when temperature exceeds 973 K due to the presence of $\text{Na}_2\text{CO}_3\text{-Na}_2\text{CrO}_4$ eutectic melt, and the higher the temperature is, the higher the conversion rate will be. But, the melting point of Na_2CrO_4 is only 1065.15 K, when temperature exceeds this value, there will be too many melting substances, and globule formation and kiln chocking problems will arise in a rotary kiln on industrial scale. So, 1023 K is optimal to other temperatures in industrial production. On the kinetic curve of 1023 K in

Fig. 5, it can be seen that the conversion rate becomes flat after roasting for 80 min, therefore, a roasting duration of 80 min has optimal economic efficiency.

3.3 Effect of carbon ferrochrome grain size

Generally, small grain size is favorable for the mass transfer process. In this part, three different grain sizes of CrFeC were investigated. The grain sizes of the three samples are shown in Table 2.

Table 2 Grain sizes of CrFeC samples

Sample No.	$D_{10}/\mu\text{m}$	$D_{50}/\mu\text{m}$	$D_{90}/\mu\text{m}$
1	3.2	17.4	34.3
2	2.3	12.6	25.4
3	1.8	9.7	19.6

All the three samples were mixed with stoichiometric Na_2CO_3 , and then, roasted at different temperatures in air for 80 min. The results in Fig. 9 show that, relatively high conversion rates are obtained for all the three samples when temperature is above 973 K, and the variation of CrFeC grain size has no obvious effect on the conversion rate above 973 K. But Sample 3 with the smallest grain size shows its advantage at 923 K, i.e., the conversion rate is far higher than that of the other two samples. This is because that small particle size can make CrFeC and Na_2CO_3 in sufficient contact and accelerate the production of Na_2CO_3 – Na_2CrO_4 eutectic melt, which is the main reason for the jump of the reaction rate. Therefore, Sample 3 with a grain size of $D_{50}=9.7 \mu\text{m}$ is more favorable to the reaction.

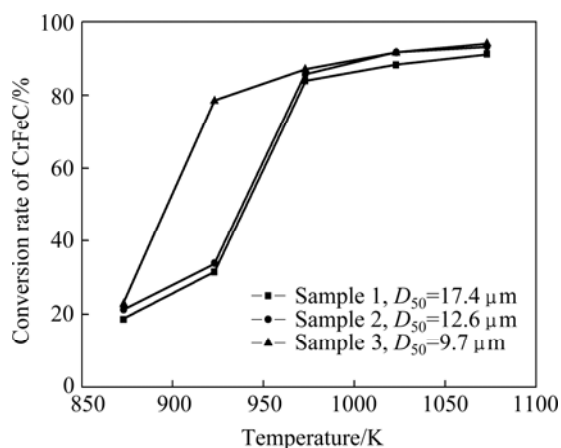


Fig. 9 Effect of CrFeC grain size on conversion rate of CrFeC

3.4 Effect of mole ratio of Na_2CO_3 to CrFeC

The effect of the mole ratio of Na_2CO_3 to CrFeC being 1:1 (stoichiometry), 1.05:1, 1.1:1, 1.15:1 and 1.2:1 on the conversion rate of CrFeC was investigated. The roasting temperature is 1023 K, roasting duration is 80 min, and the grain size of CrFeC is $D_{50}=9.7 \mu\text{m}$. The experiment results are shown in Fig. 10. It can be seen

that the conversion rate of CrFeC rises significantly with the increase of the mole ratio of Na_2CO_3 to CrFeC. The conversion rate of CrFeC is as high as 99.34% when the mole ratio of Na_2CO_3 to CrFeC reaches up to 1.2:1. This shows that sufficient Na_2CO_3 is one of the key factors to ensure quick and thorough reaction. If Na_2CO_3 is insufficient, Na^+ should migrate for larger range in order to contact with CrFeC in the later stage of the reaction, which will greatly delay the reaction rate. Accordingly, a mole ratio of Na_2CO_3 to CrFeC of 1.2:1 is optimal for the roasting reaction.

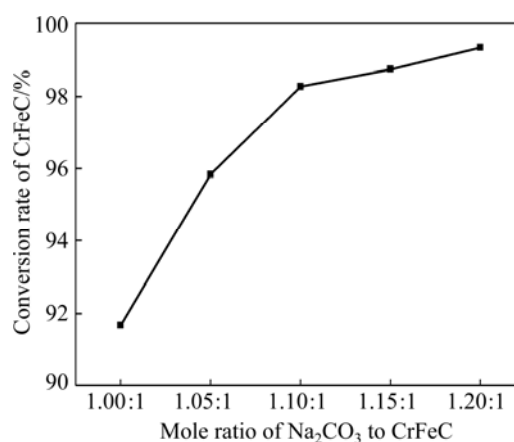


Fig. 10 Effect of mole ratio of Na_2CO_3 to CrFeC on conversion rate of CrFeC

3.5 Leaching solution and residue

A roasting product was firstly obtained under the following technological conditions: the grain size of CrFeC $D_{50}=9.7 \mu\text{m}$, mole ratio of Na_2CO_3 to CrFeC 1.2:1, roasting temperature 1023 K, roasting duration 80 min. The XRD pattern of the roasting product is shown in Fig. 11. According to the XRD pattern in Fig. 11, the roasting product mainly consists of Na_2CrO_4 , Na_4CrO_4 and Fe_2O_3 .

The roasting product was leached and washed. At last, it was filtered to get a Na_2CrO_4 solution and a chromium residue.

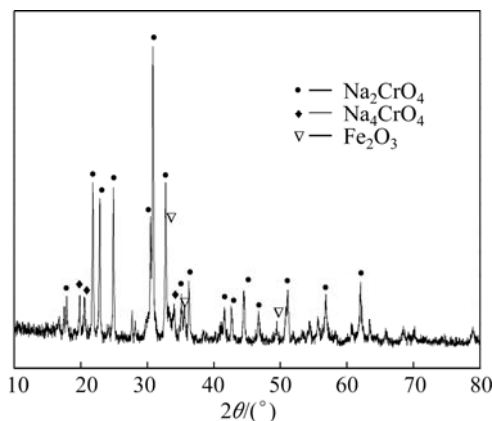


Fig. 11 XRD pattern of roasting product

The chemical components of the leaching solution are shown in Table 3. The fractions of the impurities in the solution are all quite low, namely, Na_2CrO_4 can be achieved just through a simple refining process.

Table 3 Chemical components of leaching solution (mg/L)

Cr	K	Si	Al	
3.98×10^3	4.08×10^3	8.6	10.1	
Mn	Co	V	As	Ca
2.6	1.3	2.9	2.4	1.4

The XRD pattern of the chromium residue is shown in Fig. 12. It can be seen that the residue mainly consists of Fe_2O_3 , and there are no cementitious materials like tricalcium silicate or calcium alluminoferrite in the residue. The particle size distribution in Table 4 indicates that the particle size of the residue is very small, only tens of microns. So, it is favorable for high efficient leaching of Cr(VI). Chemical analysis [14] shows that Cr(VI) remaining in the chromium residue is only 0.06%, far less than that of the traditional soda–ash roasting process, which is as high as 1%–2% [2,15]. The quantity of the residue is very little, only about 1/3 of the product, compared with 250% of the product in the soda–ash process. The Fe content in the residue reaches up to 60.41% according to a volumetric analysis [16]. So, the residue can be easily recycled to produce sponge iron by a carbon reduction method, realizing the complete detoxication of chromium residue and the target of clean production [17,18].

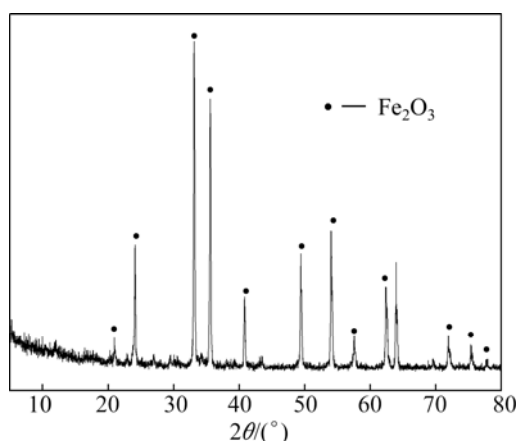


Fig. 12 XRD pattern of chromium residue

Table 4 Particle size distribution of chromium residue

$D_{10}/\mu\text{m}$	$D_{50}/\mu\text{m}$	$D_{90}/\mu\text{m}$
5.7	31.8	73.16

4 Conclusions

1) Due to the presence of Na_2CO_3 – Na_2CrO_4 eutectic

melt, an obvious jump of the reaction rate can be observed at above 973 K. In the temperature range of 873–923 K, the roasting reaction is controlled by interface chemical reaction, and the apparent activation energy is 51.85 kJ/mol. While at 973–1023 K, the reaction is controlled by external diffusion process, and the apparent activation energy is 26.53 kJ/mol.

2) CrFeC with small grain size is more favorable to the reaction. Mole ratio of Na_2CO_3 to CrFeC has a significant effect on the recovery rate of chromium, and it reaches up to 99.34% when mole ratio of Na_2CO_3 to CrFeC increases to 1.2:1.

3) The quantity of the residue is very low, only about 1/3 of the product. Moreover, this high-iron residue can be easily recycled to produce sponge iron, through which the targets of complete detoxication and zero-emission of chromium residue are realized.

References

- [1] CHENG Si-wei, DING Ji, YANG Chun-rong. Production process of chromium salts [M]. Beijing: Chemical Industry Press, 1988: 23–109. (in Chinese)
- [2] TATHAVADKAR V D, ANATONY M P, JHA A. The effect of salt-phase composition on the rate of soda–ash roasting of chromite ores [J]. Metallurgical and Materials Transactions B, 2003, 34: 555–564.
- [3] MOON D H, WAZNE M, DERMATAS D, CHRISTODOULATOS C, SANCHEZ A M, GRUBB D G. Long-term treatment issues with chromite ore processing residue (COPR): Cr^{6+} reduction and heave [J]. Journal of Hazardous Materials, 2007, 143(3): 629–635.
- [4] MEI Hai-jun, LI Xia, ZHANG Da-wei, MA Guang-hui. The advantages of cleaning production technology—“non-calcium roasting method” for chromium salt [J]. Inorganic Chemicals Industry, 2005, 37(3): 5–9. (in Chinese)
- [5] YAN Jiang-feng. Chromium metallurgy [M]. Beijing: Metallurgical Industry Press, 2007: 3–25. (in Chinese)
- [6] TAHVADKAR D, ANTONY M P, JHA A. The soda–ash roasting of chromite minerals: Kinetics [J]. Metallurgical and Materials Transactions B, 2001, 32: 593–603.
- [7] YE Da-lun, HU Jian-hua. Handbook of practical inorganic thermodynamic data [M]. 2nd ed. Beijing: Metallurgical Industry Press, 2002: 1–1208. (in Chinese)
- [8] GUO Han-jie. Metallurgical physical chemistry course [M]. Beijing: Metallurgical Industry Press, 2006: 114–126. (in Chinese)
- [9] SUN Kang. Macro-kinetics and analytical method [M]. Beijing: Metallurgical Industry Press, 1988: 1–10. (in Chinese)
- [10] LUO Shi-yong, ZHANG Jia-yun, ZHOU Tu-ping. Models for kinetic analysis of solid–solid reactions and their application [J]. Materials Leader, 2004, 14(4): 6–8.
- [11] QI Tian-gui, LIU Nan, LI Xiao-bin, PENG Zhi-hong, LIU Gui-hua, ZHOU Qiu-sheng. Thermodynamics of chromite ore oxidative roasting process [J]. Journal of Central South University, 2011, 18: 83–85.
- [12] YANG Xi-yun, GONG Zhu-qing, LIU Feng-liang. Kinetics of Fe_2O_4 formation by air oxidation [J]. Journal of Central South University, 2004, 11: 102–108.
- [13] LI Bao-shan, WANG Yong-ning, JIA Yuan-chun. The method of measuring the content of chromium sediment Cr^{6+} [J]. Journal of

- Qinghai Normal University: Natural Science, 2006, 3: 74–76. (in Chinese)
- [14] WANG Tian-gui, LI Qiang, QIN Li-ling, LI Shu-ling. Evaluation of methods for determination of hexavalent chromium contained in chromite ore processing residue [J]. Inorganic Chemicals Industry, 2012, 44(4): 1–4. (in Chinese)
- [15] LIU Wei, LI Bin, ZHOU Qiu-sheng, QI Tian-gui, PENG Zhi-hong, LIU Gui-hua, LI Xiao-bin. Thermodynamic analysis of chromite processing residue treatment in $\text{NaCO}_3\text{-CO}_2\text{-H}_2\text{O}$ system [J]. Journal of Central South University: Science and Technology, 2011, 42(5): 1209–1214. (in Chinese)
- [16] LI Xiao-bin, XU Wen-bin, ZHOU Qiu-sheng, PENG Zhi-hong, LIU Gui-hua. Leaching kinetics of acid-soluble Cr(VI) from chromite ore processing residue with hydrofluoric acid [J]. Journal of Central South University, 2011, 18: 399–405.
- [17] HUANG Zhu-cheng, CAI Ling-bo, ZHANG Yuan-bo. Study on the sponge iron preparation by direct reduction of high iron red mud by Bayer process [J]. Metal Mineral, 2009, 39(3): 173–178. (in Chinese)
- [18] SELAN M, LEHRHOFER J, FRIEDRICH K, KORDESCH K, SMADER G. Sponge iron: Economic, ecological, technical and process-specific aspects [J]. Journal of Power Sources, 1996, 61(1–2): 247–253.

一种以碳素铬铁为原料制备铬酸钠的新方法

王家良, 胡国荣, 彭忠东, 杜柯

中南大学 冶金与环境学院, 长沙 410083

摘要: 研究以碳素铬铁为原料在碳酸钠与空气的存在下经氧化焙烧制备铬酸钠的反应过程。考察反应温度、反应时间、碳酸钠与碳素铬铁的摩尔比对氧化焙烧过程的影响, 并讨论反应的热力学与动力学。结果表明, 当反应温度达到一定值时反应速度会产生明显的跃升, 粒度较小的碳素铬铁可以在较低的温度下产生反应速率的跃升。铬的回收率随碳酸钠与碳素铬铁摩尔比的增加而增大, 当碳酸钠与碳素铬铁的摩尔比为 1.2:1 时, 铬的回收率达到 99.34%。此工艺产生的铬渣量极少, 仅为所得产品质量的 1/3 左右, 且铬渣中 Fe 含量高达 60.41%, 可用于碳还原法生产海绵铁, 实现铬渣的彻底解毒和零排放。

关键词: 碳素铬铁; 铬酸钠; 氧化焙烧; 铬渣; 零排放

(Edited by Wei-ping CHEN)